Design of NW TFET biosensor for enhanced sensitivity and sensing speed by using cavity extension and additional source electrode

Deepak Soni ✉, *Dheeraj Sharma*

Nanoelectronics and VLSI Lab, Electronics and Communication Engineering Discipline, Indian Institute of Information Technology, Jabalpur 482005, India
✉ *E-mail: deepaksoni09@gmail.com*

Published in Micro & Nano Letters; Received on 27th November 2018; Revised on 14th March 2019; Accepted on 26th March 2019

A planer structure of a tunnel field effect transistor (TFET) faces many consequences of fabrication complexity and less controllability of the gate electrode over the channel. Therefore, in this Letter nanowire TFET (NW TFET) is presented for the biosensing application. For this purpose, a new design approach of NW TFET has been presented to overcome the issues of planer structure TFET and for improving sensitivity and sensing speed of the biosensor. In this concern, an addition electrode is placed around the source region and the cavity, which is generally created in the oxide region under the gate electrode, is extended towards the source oxide region. Thus, due to the presence of source electrode, additional holes are accumulated in the source surface region and forming a plasma layer of holes. Hence, abruptness at source/channel junction is created. So as the biomolecules enter into the cavity, the large variation is observed in electrostatic properties of the device due to different properties (dielectric/charge) of the biomolecules. These variations reflect as improved sensitivity of the biomolecule detector. Further to this, because of the supplementary source electrode, abrupt source/channel junction provides lower subthreshold swing, which reduces the response time of the device and increases the sensing speed of biomolecules detection.

1. Introduction: Nowadays tunneling based field effect transistor (TFET) is more promising device for ultra-low power and high-speed biosensors due to virtue of different mechanism of charge flow [1, 2], the gate voltage required is <60 mV to increase one decade of output current [3], low leakage current [4], more resistive nature towards the short channel effects, and high speed of operation in comparison of MOSFET [5]. In addition to this, for the next generation of biosensors higher sensitivity with high speed is a fundamental requirement for the detection of biomolecules. In this context, a lot of work has been reported for improving the sensitivity and sensing speed of biosensor by making the changes in tunneling regions, shape of cavity and gate electrode: Formation of N+ region or pocket [6, 7] in the P+ source region, which improves the sensitivity of the biosensor at the cost of fabrication complexity. Another approach by changing the length of the gate electrode and the shape of a cavity region [8] improvement is observed insensitivity of the biosensor up to the limited extend, and detection of a biomolecule in the ambipolar region with leaving the complexity related to the compatibility with CMOS technology [9]. Other techniques are charge plasma-based biosensor [8], hybrid nanostructures for biosensing [10], junctionless TFET for biosensing applications [11], but these techniques have their limitations.

To eradicate these issues, nanowire TFET (NW TFET) structure is the most suitable substitute to achieve higher sensitivity and sensing speed [12]. The cylindrical gate structure of TFET offers large gate equivalent, which provides superb electrostatic control over the channel region. The cylindrical shape device does not face the consequences of floating gate and corners effects. Additional features of the cylindrical shape structure are volume inversion, no carrier confined near the silicon/oxide interface, and do not have any scaling issues [13–15]. In NW TFET, a cavity is formed around the gate region, which provides a large area to accommodate biomolecules in the cavity, which is helpful for the improvement in sensitivity and sensing speed.

Still, the sensing speed needs to be improved by lowering subthreshold swing (SS) of the device and sensitivity by cavity modification. Abruptness at the source/channel junction is responsible for SS of the device. The subthreshold swing of the device can be improved by increasing the impurity concentration. Silicon material does not allow to dope the impurity beyond a certain limit; it is called material solubility limit. Due to this reason, it is not possible to dope the source silicon beyond $1 \times 10^{20}\,\mathrm{cm}^{-3}$ [16, 17]. For this purpose, an additional electrode is considered in the source electrode NW TFET (SE NW TFET) around the source region, which accumulated the additional holes from the body and creates a layer of holes near the source/channel interface for creating an abrupt junction profile. Further, proposed modification is used for improving the sensitivity of the device. In this regard, the cavity which is generally created in the gate oxide region under the gate electrode is extended towards the source oxide region to accommodate the large number of biomolecules. Hence, the biomolecules inside the source cavity impact on the abruptness of the source/channel junction of the device and offers a large variation in the output characteristics of the device. Variation in output parameters shows higher sensitivity towards biomolecule detection. Along with this, NW TFET has no fabrication complexity, the nanowire can be fabricated by using either bottom-up or top-down methods [18]. In the top-down fabrication by applying CMOS-compatible conventional optical lithography with anisotropic wet etching using tetramethylammonium hydroxide, the reproducible and well-controlled NW-TFET devices can be manufactured which is the low-cost, CMOS-compatible fabrication approach. The remaining part of this Letter is organised as follows. Section 2 explains the architecture of the device and simulation setup. Section 3 describes the results and discussion. Finally, Sections 4 summaries the Letter with highlights.

2. Device structure and simulation parameter: Fig. 1*a* shows the device three-dimensional (3D) view of conventional NW TFET (C NW TFET) biosensor and Fig. 1*b* shows the cross-section view of the same (C NW TFET) device. The 3D view of proposed device SE NW TFET biosensor and its cross-sectional view is illustrated in Figs. 1*c* and *d*, respectively and other design parameters are shown in Table 1. For simulations, 3D TCAD Silvaco [19] is used. Various models such as Shockley–Read–Hall (SRH) model and Auger recombination model, Kane's model for local band-to-band tunneling (BTBT, bandgap narrowing model [20],

© The Institution of Engineering and Technology 2019

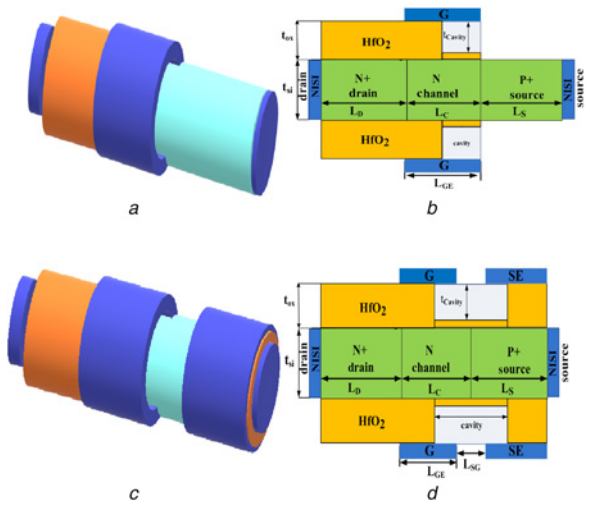


Fig. 1 *Structural view of devices*
a 3D view of C NW TFET biosensor
b Cross-sectional view of C NW TFET biosensor
c 3D view of SE NW TFET biosensor
d Cross-sectional view of SE NW TFET biosensor

Table 1 Parameter used for simulation

Parameters	Symbols	NW TFET	SE NW TFET
drain doping, cm^{-3}	N_A	1×10^{20}	1×10^{20}
source doping, cm^{-3}	N_D	1×10^{20}	1×10^{20}
channel doping, cm^{-3}	N_A	1×10^{17}	1×10^{17}
drain length, nm	L_D	100	100
source length, nm	L_S	100	100
channel length, nm	L_C	50	50
silicon thickness, nm	t_{si}	10	10
oxide thickness, nm	t_{ox}	6	6
gate to source electrode space, nm	L_{SG}	—	12
gate electrode length, nm	L_{GE}	50	44
source electrode length, nm	L_{SE}	—	94
gate electrode work function, eV	ϕ_G	4.5	4.5
source electrode work function, eV	ϕ_{SE}	—	4.5
voltage at source electrode, V	V_{SE}	—	−1.2
length of cavity, nm	L_{Cavity}	15	25
height of cavity, nm	t_{Cavity}	5.5	5.5

field mobility (Fldmob) and Fermi-Dirac statistics for analysis of the device characteristics.

3. Results and discussion

3.1. Working principle of the device and effect of the proposed modification: The carrier transport mechanism of TFET is based on BTBT phenomenon, in which the electrons penetrate the barrier at source/channel junction and enter into the conduction band of channels from the valance band of the source region. The ON state current increases as the probability of tunnelling of charge carriers at source/channel interface increases with a decrease in barrier width. Therefore, for the suppression of the barrier width and create steeper source/channel junction, higher doping of impurity in the source region is an effective technique.

However, the increment of physical doing beyond a certain limit (1×10^{20} cm^{-3}) is restricted in the semiconductor substrate due to material solubility and higher doping also degrades the mobility of charge carriers. In this regards, an approach is adopted and the additional electrode is mounted around the source region. This source electrode accumulates the holes and increases the concentration of holes in the source region at the silicon/oxide interface near to the source/channel junction as shown in Fig. 2*a*. These additional holes create an abrupt junction profile and steep band bending at the junction as depicted in Fig. 2*b*. Steep band bending reduces the barrier width and improves the electrostatic characteristics of the device due to the higher tunnelling probability of the charge carrier.

Further, this concept is used for the improvement of the sensitivity in SE NW TFET biosensor. For this purpose, the cavity is extended from the gate oxide region to source oxide region. Thus the additional biomolecules entered into the source cavity region and increased the coupling between source electrode/silicon substrate and changes the electrostatic characteristics of the device. Along with this, due to the cylindrical region of cavity biomolecule have large entering space; hence, the sensitivity of SE NW TFET is higher in comparison to C NW TFET.

3.2. Performance analysis of C NW TFET biosensor with dielectric/charge variation in the cavity region: In this section, we have presented the impact of variation of different dielectric/charges of biomolecules on the electrostatic characteristics of C NW TFET biosensor, where the cavity is formed in the gate oxide region of C NW TFET. Fig. 3*a* shows the impact of a different dielectric biomolecule in the cavity on I_{ds}–V_{gs} characteristics, as the dielectric constant, is increasing due to different biomolecules, so, ON-state current of the devices increasing and showing enough variation in the input characteristics which can be considerable change. Due to the presence of biomolecules, the same variation is observed in the output characteristic of C NW TFET biosensor as depicted in Fig. 3*b*.

The sensitivity of the biosensor device is the main design parameter, to calculate the sensitivity of the device with dielectric variation in the cavity on input/output characteristics is calculated as [21]

$$S_{I_{ds}} = \left(\frac{I_{D,\text{bio}} - I_{D,\text{air}}}{I_{D,\text{air}}} \right) \quad (1)$$

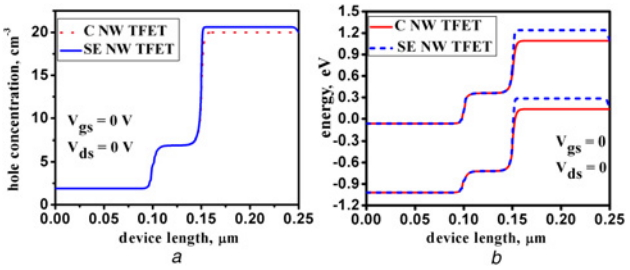


Fig. 2 *Response of the devices in thermal state*
a Hole concentration in the thermal state for both the devices
b Energy band diagram of both devices in the thermal state

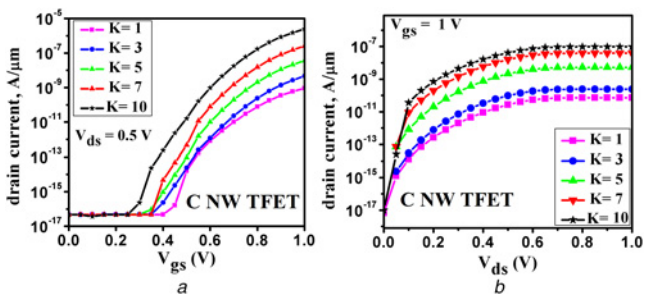


Fig. 3 *Effect of dielectric variation on*
a I_{ds}–V_{gs} characteristics for C NW TFET
b I_{ds}–V_{ds} characteristics for C NW TFET

© The Institution of Engineering and Technology 2019

doi: 10.1049/mnl.2018.5733

Figs. 4*a* and *b* show the sensitivity of the biomolecule detector is in the range of 10^{-1}–10^{3} for I_{ds}–V_{gs} and same sensitivity variation is observed in I_{ds}–V_{ds} sensitivity.

Now by changing the biomolecules of different charges in the cavity region, input/output characteristics are carried out. Figs. 5*a* and *b* show the input/output characteristics of C NW TFET biosensor and demonstrates that as the charges in the cavity region changes, it changes the ON sate current. As the charge changes, according to their polarity, these charges generate the opposite charges in the substrate and the changes in the concentration of charge, hence the changes in electrostatic characteristics of the device. The sensitivity of C NW TFET biosensor is calculated from formula (1). Figs. 6*a* and *b* show the sensitivity of C NW TFET biosensor against the variation of charges of biomolecules in I_{ds}–V_{gs} and I_{ds}–V_{ds} characteristics. From Fig. 6*a*, I_{ds}–V_{gs} sensitivity is in the range of 10^{-1}–10^{2} and from Fig. 6*b*, it can be analysed that I_{ds}–V_{ds} sensitivity lies between 10^{1} and 10^{2}.

3.3. Performance analysis of SE NW TFET biosensor with dielectric/charge variation in the cavity region: From the above-mentioned analysis, we can state that C NW TFET biosensor has sensitivity towards the biomolecules having different charge/dielectric constant. Still, the improvement can be made to upgrade sensitivity and its sensing speed. Thus, to show the improved sensitivity and sensing speed various parameters are carried out with the variation of dielectric/charges of biomolecules in the following section with the modified structure of NW TFET.

In Fig. 7*a*, the surface potential of the device is depicted for different biomolecules which distinguishing properties of dielectric constant. Due to the same reason, the surface potential is low for the biomolecule which is having low dielectric. As the constant dielectric increases, the surface potential of the device in the channel region increases. Further, the impact of charges of biomolecules which are considered in the cavity is shown in Fig. 7*b*. From the above mentioned characteristics, it is understood that as the surface potential increases band bending must be more for different dielectric constants at the junction which is depicted in Figs. 8*a* and *b* for different values of charges of biomolecules. As the surface potential increases with increase in dielectric/charges, it pushes the energy bands of channel region more and more. As the energy bands at the source/channel junction are pushes downwards and reduce the tunnelling barrier width, so the tunnelling probability of the electrons increases which is demonstrated in Fig. 9*a*. From the same Fig. 9*a* (inset), it can be referred that as the electron tunnelling rate increases it increases ON state current. The variation in the electron tunnelling rate concerning biomolecule charges is shown in Fig. 9*b*.

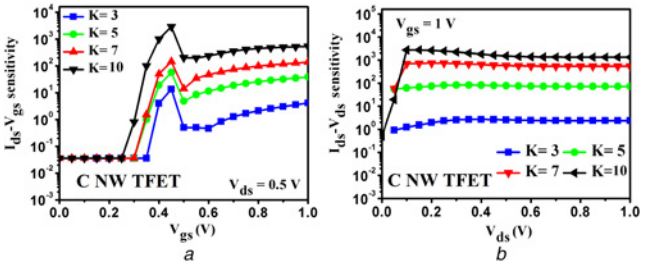


Fig. 4 *Effect of dielectric variation on*
a I_{ds}–V_{gs} sensitivity for C NW TFET
b I_{ds}–V_{ds} sensitivity for C NW TFET

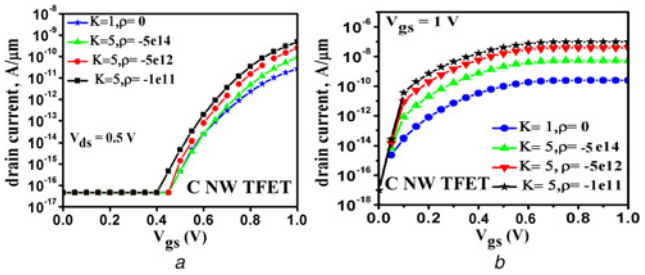


Fig. 5 *Effect of charge variation on*
a I_{ds}–V_{gs} characteristics for C NW TFET
b I_{ds}–V_{ds} characteristics for C NW TFET

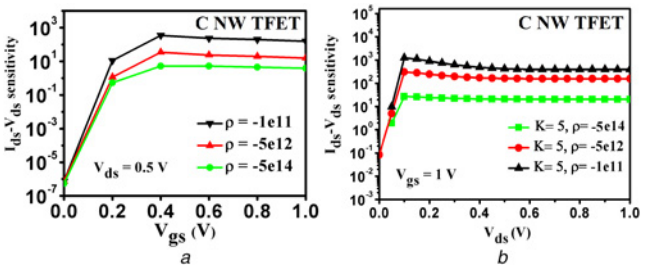


Fig. 6 *Effect of charge variation on*
a I_{ds}-V_{gs} sensitivity for C NW TFET
b I_{ds}–V_{ds} sensitivity for C NW TFET

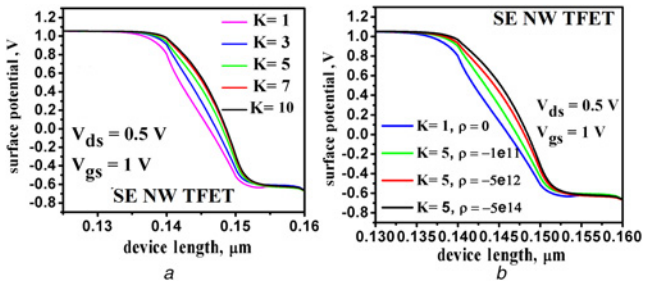


Fig. 7 *For SE NW TFET*
a Effect of dielectric variation on surface potential
b Effect of charge variation on the surface potential

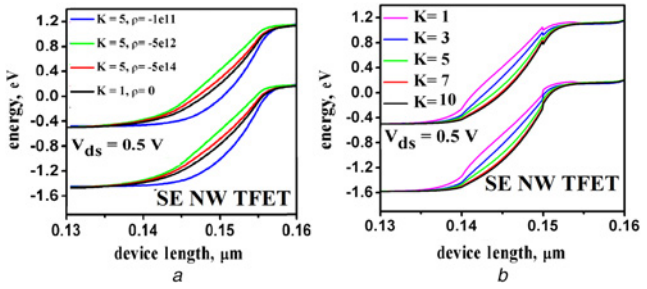


Fig. 8 *For SE NW TFET*
a Effect of dielectric variation on energy band diagram
b Effect of charge variation on energy band diagram

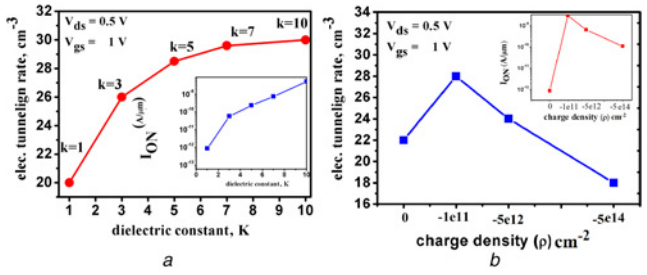


Fig. 9 *For SE NW TFET*
a Effect of dielectric variation on electron tunneling rate
b Effect of charge variation on electron tunneling rate

© The Institution of Engineering and Technology 2019

To show the impact more clearly on the electrostatic characteristics of the device for different dielectric constants of biomolecules, Fig. 10*a* shows the I_{ds}–V_{gs} characteristics. Here it can be determined that the variations in ON state current (I_{ds}) are large enough that can be identified very easily. Large variation in ON state current shows high sensitivity and higher selectivity. The variation in the I_{ds}–V_{gs} characteristics in Fig. 10*a* indicates that the deviation in ON state current of SE NW TFET is large in comparison to C NW TFET as different dielectric biomolecules are present in the cavity. Along with this, I_{ds}–V_{gs} characteristics for different charge biomolecules are shown in Fig. 10*b*.

The impact of different dielectric constant (K) is also depicted on the output characteristics of the device in Fig. 11*a*, here it can be seen that the variation in the output current is large as the dielectric constant varies. The output current shows the variation of seven decades due to different biomolecules of different dielectric constants. Output characteristics with the variation of charges are shown in Fig. 11*b* and it is showing eight decades of variation in output characteristics, this variation is large enough to identify the changes which illustrate the high sensitivity towards the charged biomolecules. Figs. 12*a* and *b* demonstrate the sensitivity for dielectric and charged biomolecule variations; in this Letter, we have calculated the sensitivity of different dielectric/charge concerning air present in the cavity. Biomolecules are having a higher dielectric constant show 10^3–10^8 sensitivity for different values of dielectric constant and charges. These results show a higher sensitivity of SE NE TFET in comparison to C NE TFET. Further, Figs. 13*a* and *b* show the sensitivity of the output current characteristics, in Fig. 13*a* the output current shows 10^3–10^8 times increment for higher values of dielectric constants (3, 5, 7, 10) in comparison to the current which is in the presence of the air ($K = 1$). A higher degree of sensitivity shows the high level of selectivity of biomolecules which is in comparison to C NW TFET. It means, different types of biomolecules which have different dielectric/charges can be easily recognised.

Furthermore, for the designing of biomolecule detectors, one more parameter is very important, which is sensing the speed of the device. Sensing speed of the device shows that how fast biomolecules can be identified in the cavity region. For this SS of the device must be as low as possible.

If the SS is low, it is required low voltage variation in input to change one decade of output current. Therefore, as the surface potential changes in the channel region due to the change in the property (dielectric constant/charge) of biomolecules, it shows the immediate effect over the output current characteristics and illustrates the high sensing speed towards the detection of biomolecules. If SS of the device is higher, then it will require large voltage variation in the input for changing output current and it will take more time to show the variation in output current. In SE NW TFET due to additional electrode source/channel junction is abrupt and provides low SS which is helpful to achieve higher sensing speed. To show the speed of the presented structure of the biosensor SS for the different dielectric constant is extracted and depicted in Fig. 14*a*, here it can be visualised that as the biomolecules of higher dielectric constant increasing in the cavity region SS of the device is decreasing. Fig. 14*b* shows the sensitivity of the device in terms of SS. SS and SS sensitivity of the device for the differently charged biomolecule in the cavity are presented in Fig. 15.

Fig. 16*a* shows the current ratio of I_{ON} and I_{OFF} for the confirmation of higher sensitivity of SE NW TFET biosensor, here it can be noticed that ratio for different dielectric constant is increasing, it

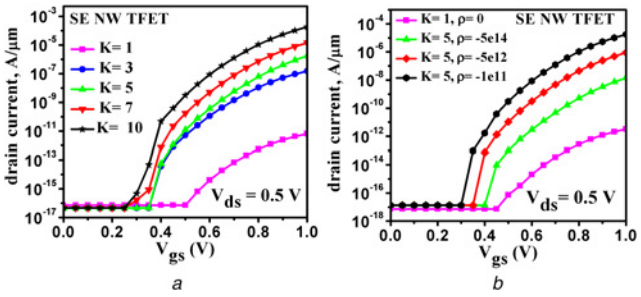


Fig. 10 *For SE NW TFET*
a Effect of dielectric variation on I_{ds}–V_{gs} characteristics
b Effect of charge variation on I_{ds}–V_{gs} characteristics

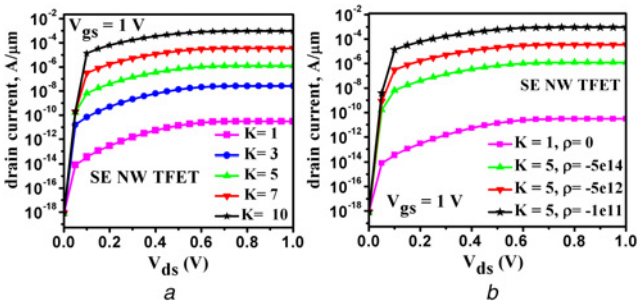


Fig. 11 *For SE NW TFET*
a Effect of dielectric variation on I_{ds}–V_{ds} characteristics
b Effect of charge variation on I_{ds}–V_{ds} characteristics

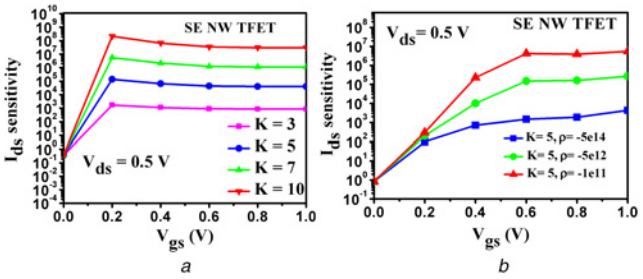


Fig. 12 *Sensitivity of SE NW TFET in terms of I_{ds}-V_{gs} characteristics*
a For different dielectric constant
b For different charge density

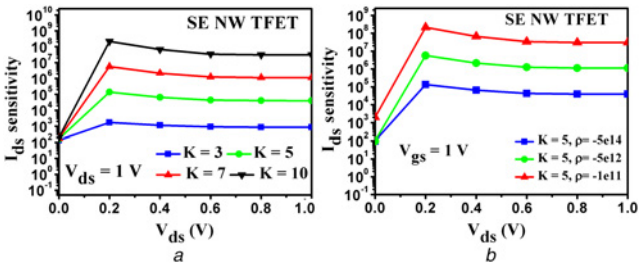


Fig. 13 *Sensitivity of SE NW TFET in terms of I_{ds}-V_{ds} characteristics*
a For different dielectric constant
b For different charge density

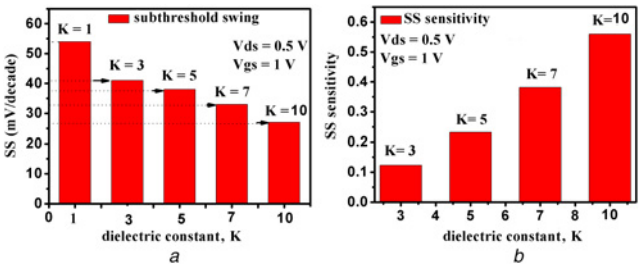


Fig. 14 *For SE NW TFET*
a Effect of dielectric variation on SS for both devices
b SS sensitivity for different dielectric constant

© The Institution of Engineering and Technology 2019

doi: 10.1049/mnl.2018.5733

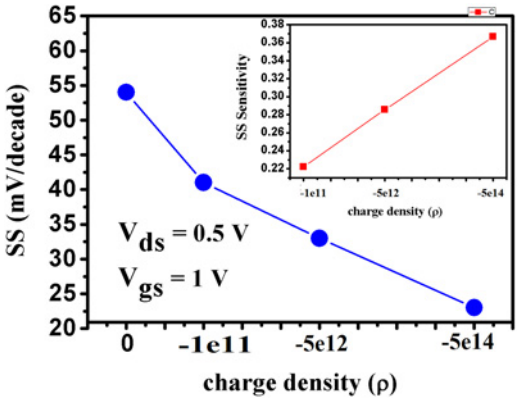


Fig. 15 *For SE NW TFET*
a Effect of charge variation on SS for different charge density
b SS sensitivity for different charge density

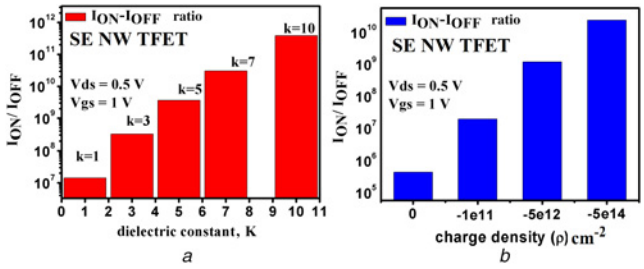


Fig. 16 *For SE NW TFET*
a I_{ON}–I_{OFF} ratio for different dielectric constant
b I_{ON}–I_{OFF} ratio for different charge density

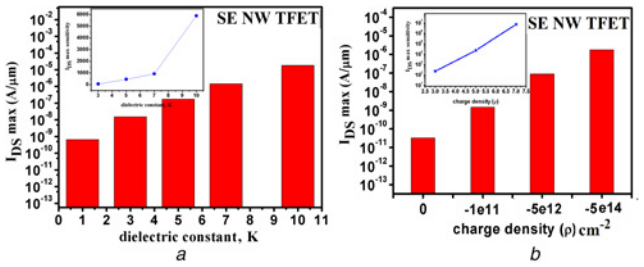


Fig. 17 *Variation in I_{DSmax} and sensitivity in SE NW TFET*
a For different dielectric constant
b For different charge density

means, off-state current is constant and on-state current is increasing significantly. Thus, it can be stated that SE NW TFET shows higher sensitivity. Similarly, for different charges, the device shows large variation in current ratio, which is easy can be recognised and shows the high sensitivity of the device towards the variation of charges in the cavity region. Further, to show the sensitivity the changes must be identified on the output parameter of the device. Therefore, we have presented a plot of maximum output current for different dielectric constant and maximum output current for different charges in Figs. 17*a* and *b*. From these figures, it can be recognised that as the biomolecules of higher dielectric constant increases, the output current will change significantly and show a high level of sensitivity shown in Fig. 17*a* (inset). Similarly, the effect of charge density variation in the cavity region on maximum current and sensitivity is shown in Fig. 17*b*.

4. Conclusion: In this Letter, we have proposed a SE NW TFET for biomolecule detector with a new concept of cavity design for the improvement of the selectivity of biomolecules and sensing speed. By the variation of different dielectric constant/charges density, it is found that the proposed devices show large variations in the electrostatic characteristics. The device sensitivity is in the range of 10^3–10^8 by overcoming the solubility limit of the silicon. Further, the stretched cavity in the source oxide region improved sensing speed of SE NW TFET biosensor.

5 References

[1] Boucart K., Ionescu A.M.: 'Silicon nanowire tunnelling field-effect transistors', *IEEE Trans. Electron Devices*, 2007, **54**, (7), pp. 1725–1733
[2] Boucart K., Riess W., Ionescu A.M.: 'Lateral strain profile as key technology booster for all-silicon tunnel FETs', *IEEE Electron Device Lett.*, 2009, **30**, (6), pp. 656–658
[3] Zhang Q., Zhao W., Seabaugh A.: 'Low-subthreshold-swing tunnel transistors', *IEEE Electron Device Lett.*, 2006, **27**, (4), pp. 297–300
[4] Koswatta S.O., Lundstrom M.S., Nikonov D.E.: 'Performance comparison between p-i-n tunneling transistors and conventional MOSFETs', *IEEE Trans. Electron Devices*, 2007, **56**, (3), pp. 456–465
[5] Bangsaruntip S., Cohen G.M., Majumdar A., *ET AL.*: 'Universality of short-channel effects in undoped-body silicon nanowire MOSFETs', *IEEE Electron Device Lett.*, 2010, **31**, (9), pp. 903–905
[6] Verma M., Tirkey S., Yadav S., *ET AL.*: 'Performance assessment of a novel vertical dielectrically modulated TFET-based biosensor', *IEEE Trans. Electron Devices*, 2017, **63**, (9), pp. 3841–3848
[7] Kanungo S., Chattopadhyay S., Gupta P.S., *ET AL.*: 'Study and analysis of the effects of SiGe source and pocket-doped channel on sensing performance of dielectrically modulated tunnel FET-based biosensors', *IEEE Trans. Electron Devices*, 2016, **63**, (6), pp. 2589–2596
[8] Kanungo S., Chattopadhyay S., Gupta P.S., *ET AL.*: 'Comparative performance analysis of the dielectrically modulated full gate and short-gate tunnel FET-based biosensors', *IEEE Trans. Electron Devices*, 2015, **62**, (3), pp. 994–1001
[9] Abdi D.B., Kumar M.J.: 'Dielectric modulated overlapping gate-on-drain tunnel-FET as a label-free biosensor', *Superlattices Microstruct.*, 2015, **86**, pp. 198–202
[10] Zhang S., Geryak R., Geldmeier J., *ET AL.*: 'Synthesis, assembly, and applications of hybrid nanostructures for biosensing', *Chem. Rev.*, 2017, **117**, pp. 12942–13038
[11] Parihar M.S., Kranti A.: 'Enhanced sensitivity of double gate junctionless transistor architecture for biosensing applications', *Nanotechnology*, 2015, **26**, (14), pp. 1–8
[12] Gao X.P.A., Zheng G., Lieber C.M.: 'Subthreshold regime has the optimal sensitivity for nanowire FET biosensors', *Nano Lett.*, 2010, **10**, (2), pp. 547–552
[13] Sharma D., Vishvakarma S.K.: 'Precise analytical model for short channel cylindrical gate (CylG) gate-All-around (GAA) MOSFET', *Solid-State Electron.*, 2013, **86**, pp. 68–74
[14] Gandhi R., Chen Z., Singh N., *ET AL.*: 'Vertical Si-nanowire n-type tunneling FETs with at room temperature', *IEEE Electron Device Lett.*, 2011, **32**, (4), pp. 437–439
[15] Vishnoi R., Jagadesh Kumar M.: 'Compact analytical drain current model of gate-all-around nanowire tunneling FET', *IEEE Trans. Electron Devices*, 2014, **61**, (7), pp. 2599–2603
[16] Schmid H., Bjrk M.T., Knoch J., *ET AL.*: 'Doping limits of grown in situ doped silicon nanowires using phosphine', *Nano Lett.*, 2009, **57**, (4), pp. 820–826
[17] Knoch J., Muller M.R.: 'Electrostatic doping controlling the properties of carbon-based FETs with gates', *IEEE Trans. Nanotechnol.*, 2014, **13**, (6), pp. 1044–1052
[18] Gao A., Lu N., Wang Y., *ET AL.*: 'Robust ultrasensitive tunneling-FET biosensor for point-of-care diagnostics', *Sci. Rep.*, 2016, doi: org/10.1038/srep22554
[19] Silvaco International: ATLAS device simulation software, Silvaco International, Santa Clara, CA, USA, 2012
[20] Awadhiya B., Pandey S., Nigam K., *ET AL.*: 'Effect of ITCs on linearity and distortion performance of Junctionless tunnel field effect transistor', *Superlattices Microstruct.*, 2017, **111**, (3), pp. 293–301
[21] Narang R., Saxena M., Gupta M.: 'Comparative analysis of dielectric-modulated FET and TFET-based biosensor', *IEEE Trans. Electron Devices*, 2015, **14**, (3), pp. 427–435

© The Institution of Engineering and Technology 2019